Crystal structure of the superconducting layered cobaltate $Na_xCoO_2 \cdot yD_2O$

Crystal structure of the superconducting layered cobaltate Na$_x$CoO$_2$·yD$_2$O

D N Argyriou[1,4]**, P G Radaelli**[2]**, C J Milne**[1]**, N Aliouane**[1]**, L C Chapon**[2]**,
A Chemseddine**[1]**, J Veira**[1]**, S Cox**[3]**, N D Mathur**[3] **and P A Midgley**[3]

[1] Hahn-Meitner-Institut, Glienicker Straße 100, Berlin D-14109, Germany
[2] ISIS Facility, Rutherford Appleton Laboratory—CCLRC, Chilton, Didcot, Oxfordshire
OX11 0QX, UK
[3] Department of Materials Science and Metallurgy, University of Cambridge, Pembroke Street,
Cambridge CB2 3QZ, UK

E-mail: argyriou@hmi.de

Abstract

We have used electron diffraction and neutron powder diffraction to elucidate
the structural properties of superconducting Na$_x$CoO$_2$·yD$_2$O over a wide
compositional range. Our measurements show that superconducting samples
exhibit a number of supercells ranging from $\frac{1}{3}a^*$ to $\frac{1}{15}a^*$, but the predominant
modulation, observed also in the neutron data, is a double hexagonal cell with
dimensions $2a \times 2a \times c$. Rietveld analysis reveals that D$_2$O is inserted between
CoO$_2$ sheets to form a layered network of NaO$_6$ triangular prisms. Our model
removes the need to invoke a 5 K superconducting point compound and suggests
that a solid solution of Na is possible within a relatively constant amount of
water y.

(Some figures in this article are in colour only in the electronic version)

1. Introduction

The tuning of the Na content in the alkali layered cobaltate Na$_x$CoO$_2$ results in remarkable
changes in its physical behaviour, ranging from magnetothermoelectricity at $x = 0.75$ [1] to
charge ordering at $x = 0.5$ [2, 3] and 5 K superconductivity at $x = 0.3$ after intercalation
of H$_2$O [4]. This interesting combination of physical phenomena occurs within a structural
motif reminiscent of geometrically frustrated systems. Here, CoO$_2$ sheets are constructed by
edge sharing CoO$_6$ octahedra, forming a quasi-2D triangular net. The exact mechanism of
superconductivity within this triangular motif is currently a topic of extensive scientific inquiry,
as it holds the possibility of realizing Anderson's resonating valence bond model.

_____

[4] Author to whom any correspondence should be addressed.

For superconducting $Na_xCoO_2 \cdot yH_2O$, two mutually incompatible structural models have been proposed to date [5, 6]. The model proposed by Lynn *et al* asserts that the intercalated water assumes a structure similar to that of *ice* [5] in between the CoO_2 sheets, whereas that proposed by Jorgensen *et al* suggests a coordination and crystal chemical linkage between Na and H_2O similar to that found in many alkali hydrate systems [6]. Both structural models imply that the Na concentration x and the amount of intercalated water y are intimately related. Jorgensen's model also implies that *optimal* T_C corresponds to a line compound exhibiting full Na and D_2O ordering with a Na/H_2O ratio $\sim 1/4$ [6]. Both models are based on the parent structure and unit cell, and rely heavily on chemical constraints for interpreting the multiple symmetry-equivalent water sites in that cell. In spite of their complexity, these models do not reproduce some important aspects of the neutron diffraction data. In particular, an intense Bragg peak at (2.8 Å), and a broad distribution of intensity around (~ 2.6 Å) are not accounted for, although Jorgensen *et al* speculate that both features may result from a larger periodicity [6].

The crystal structure of this superconductor is complicated further by the recent revision of its stoichiometry [7], to account for a Co oxidation state lower than that expected if the system is doped purely with Na non-stoichiometry. This work suggests that charge neutrality is reached by the intercalation of oxonium ions (H_3O^+) along with water, giving a composition of this superconducting phase of $Na_{0.337}(H_3O)_{0.234}CoO_2 \cdot yH_2O$ [7]. In a recent examination of the superconducting phase diagram of $Na_x(H_3O)_zCoO_2 \cdot yH_2O$, we accounted for the Co oxidation state via redox titrations, and demonstrated that the optimal T_C for this superconductor is obtained over a wide Co valence range, 3.24–3.35, while T_C decreases for samples with Co valence >3.35. These measurements show that this layered superconductor is hole doped with respect to Co^{3+}, contrary to initial reports of electron doping with respect to Co^{4+} if Na content alone controls the electronic doping [8]. Although the Co valence states for superconducting compositions have now been clearly established [7, 9, 10], the evidence for the intercalation of H_3O^+ into the lattice is largely based on the hardening of certain Na Raman modes, leading Takada *et al* to suggest that H_3O^+ ions reside on Na sites [7]. This does not constitute a direct observation of H_3O^+ in the $Na_xCoO_2 \cdot yH_2O$ lattice, and the issue of how exactly these materials are doped remains largely open. It is worth noting that the structural models of Jorgensen *et al* and Lynn *et al* do not provide a structural picture for the possible intercalation of H_3O^+.

To unravel the complexity of its crystal structure and gain insight into parameters that are critical in establishing a superconducting phase, we clearly need to establish the true translational symmetry of $Na_xCoO_2 \cdot yH_2O$. To this end, we have performed electron diffraction (ED) and neutron powder diffraction (NPD) measurements, the latter employing isotopic H–D substitutions. Both sets of data clearly establish that Na and D_2O order in the structure of the superconducting phase resulting in a *doubling* of the hexagonal unit cell along both a and b. Our analysis shows that Na atoms are coordinated by D_2O forming an ordered network of NaO_6 triangular prisms. This model can account well for the intense Bragg reflection in the neutron data at ~ 2.8 Å. The ED also shows a number of different superstructures, suggesting significant Na inhomogeneities. These additional ordering modes are most probably the origin of a broad distribution of scattered intensity at ~ 2.6 Å, a common feature of all the neutron data published thus far. Our double-cell model is able to accommodate a variable amount of Na within the same water framework, strongly suggesting that $Na_xCoO_2 \cdot yH_2O$ is *not* a line compound.

2. Experimental details

In this work four different superconducting samples were investigated with varying Na content x, from $x = 0.41$ to 0.32. Details of the synthesis and characterization of these materials are
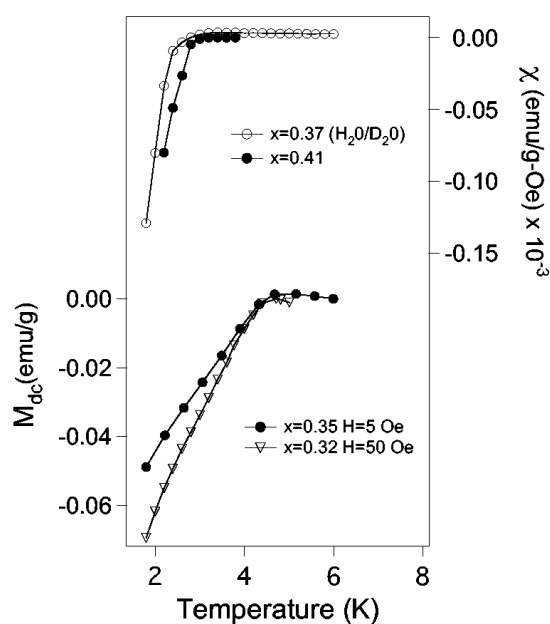
Figure 1. Zero-field cooled dc magnetization and susceptibility measurements of the two samples used in the NPD and ED experiments.

Table 1. Details of the preparation, hydration medium and characterization of the samples used in this work. The oxidation state of Co was determined from redox titrations. The superconducting transition temperatures, T_C, were determined using a SQUID magnetometer, defining T_C as the onset of diamagnetism in zero-field cooled measurements with $H = 50$ or 150 Oe. Lattice constants are determined from Rietveld analysis of x-ray powder diffraction data at room temperature. Details of sample preparation and characterization are found in [9].

Br excess	x	$Co^{\alpha+}$	H_2O/D_2O	a (Å)	c (Å)	c/a	T_C
2	0.41	3.38	D_2O	2.8278(14)	19.561(2)	6.917(10)	2.8
5	0.37	3.45	$(H, D)_2O$	2.8257(8)	19.578(7)	6.928(6)	2.5
5	0.35	3.24	D_2O	2.8253(11)	19.676(8)	6.971(8)	4.7
36	0.32	3.27	D_2O	2.8231(10)	19.784(7)	7.008(7)	4.5

found elsewhere [9]. The Na/Co ratio of these samples was measured using neutron activation analysis (NAA) to establish x. The Co valence was measured directly by redox titration as described in [7, 9]. The crystal structure of these materials was checked prior to the neutron diffraction experiments, using a Guinier x-ray diffractometer (XRD) with a Cu Kα source which confirmed that all samples crystallized in a hexagonal structure as described by Takada *et al* [4] and were free of intermediate hydrate or anhydrous Na_xCoO_2 phases. Superconducting properties were characterized using a Quantum Design SQUID magnetometer and are shown in figure 1. Strong diamagnetic signals were observed for the $x = 0.35$ and 0.32 samples. For the lower T_C samples $x = 0.41$ and 0.37, weaker diamagnetic signals were found and the superconducting transition was determined by measuring M versus H as a function of temperature and computing χ from linear fits to the data. In table 1 we give a summary of our results from the characterization of our samples in terms of Na content x, Co oxidation state, lattice constants and superconducting transition temperatures.
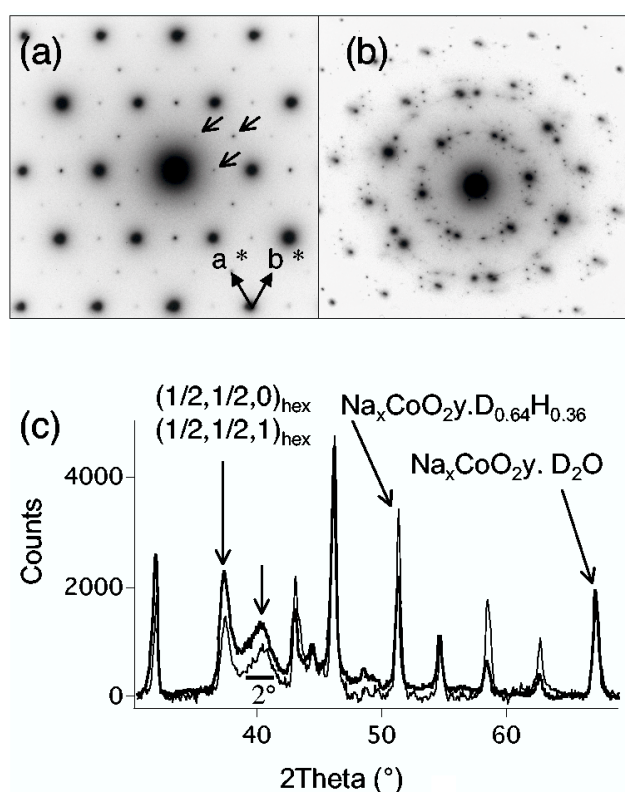
Figure 2. (a), (b) ED patterns from $Na_{0.35}CoO_2 \cdot yD_2O$. The arrows in (a) indicate the cell doubling reflections. (c) A portion of the neutron diffractogram from the $Na_{0.35}CoO_2 \cdot yD_2O$ with $T_C = 4.7$ K (heavy line) and $Na_{0.35}CoO_2 \cdot y(H_{0.641}D_{0.359})_2O$ (light line) samples. The background arising from the incoherent neutron scattering from H atoms has been subtracted. The $(\frac{1}{2}, \frac{1}{2}, 0)$, $(\frac{1}{2}, \frac{1}{2}, 1)$ doublet is indicated, as well as the broad feature at $40°$.

ED patterns of these samples were taken using a Philips CM30 transmission electron microscope operated at 300 kV with the sample cooled to approximately 90 K using a Gatan double-tilt liquid nitrogen stage. NPD data were measured from these polycrystalline samples at 2 K using the high resolution powder diffractometer E9 ($\lambda = 1.7973$ Å), located at the Berlin Neutron Scattering Centre, at the Hahn-Meitner-Institut. Additional data were collected on samples of varying x on the GEM diffractometer at ISIS, which were critical in developing the present model, and will be presented elsewhere. To locate the O atoms of the water molecules, the sample with $T_C = 2.8$ K that was originally hydrated with D_2O was exposed to a $(H_2O)_{0.641}(D_2O)_{0.359}$ moisture mixture at a temperature of 26 °C for three days. This isotopic H/D ratio gives a zero mean coherent neutron scattering length for protons ($\overline{b}_H = -0.374$, $\overline{b}_D = 0.667$), so in principle for this sample the contribution of protons to the entire diffraction pattern can be ignored. A comparison of NPD measurements between this sample and a fully deuterated sample is shown in figure 2.

3. Structural solution and refinement

Our ED measurements show that the *average* symmetry of the superconducting compound remains hexagonal everywhere. In the majority of grains, superlattice reflections indicate a

cell doubling giving an average unit cell of $2a \times 2a \times c$ (see figure 2(a)) where a and c are the lattice constants of the parent $P6_3/mmc$ hexagonal cell. Examination of the NPD data shows that the strong reflection observed at 37° (2.8 Å) can be assigned to the $(\frac{1}{2}, \frac{1}{2}, 0)$, $(\frac{1}{2}, \frac{1}{2}, 1)$ Bragg peaks, as shown in figure 2(c). We can construct a chemically sensible double-cell structural model that fits the 2.8 Å peak, providing the strongest indication that this and the ED superlattice reflections have the same origin. Further investigation of the ED data reveals an even more complex superstructure in some areas of the sample as seen in figure 2(b). Satellite reflections, decorating the parent hexagonal lattice reflections, are arranged in hexagonal nets with **q**-vectors whose magnitude have been found to vary from $(1/15)\mathbf{a}^*$ to $(1/3)\mathbf{a}^*$, but whose direction is always parallel or nearly parallel to $\langle 110 \rangle^*$. The example shown in figure 2(b) corresponds to a supercell translation vector of $3a + 3\frac{2}{3}b$, requiring a *discommensuration* to allow registry between the supercells, equivalent to the Na1–Na2 interatomic vector (see below). In all such patterns mirror symmetry perpendicular to the basal planes is broken, as seen from the gross asymmetry in the intensities of satellite reflections of type $\mathbf{g} \pm \mathbf{q}$ (where **g** is a reciprocal lattice vector). However, the sixfold symmetry appears to be conserved throughout. The detailed superstructure of these modulated phases will be discussed further in a forthcoming publication.

These more complex superstructures seen in the ED measurements are not clearly observed in our NPD data. Indeed, an examination of the NPD data does not show the presence of any additional superlattice reflections above 37°, suggesting that disorder (which we model as a large effective Debye–Waller factor for water) is substantially attenuating their intensity (superstructure reflections in ED are enhanced due to dynamical diffraction). Comparison of the diffractograms from our deuterated and isotopically mixed HD samples show appreciable differences as illustrated in the inset of figure 2(c). While some reflections show no significant change in their intensity with the isotopic substitution (for example $2\theta \sim 31°$ and 37°), others do. That the intensity of the superlattice reflections at 37° as well as the broad feature at 40° is changed, indicates that their structure factor has an appreciable contribution from protons. The origin of the broad diffuse feature at 40° (2.6 Å) is controversial as it has been described either as an impurity phase [5] or a broad Bragg reflection [6]. We argue below that it may arise from a superposition of Bragg peaks from the additional ordering modes and from short range order. To eliminate the effect of this broad feature to the fitting of the background in our Rietveld analysis, the background was interpolated through the entire diffraction pattern and to include this broad feature. The interpolated background is shown in figure 3.

To construct a structural model of the $Na_xCoO_2 \cdot yD_2O$ superconductor we analysed the NPD data using a double hexagonal unit cell $(2a \times 2a \times c)$. The space group was identified as $P6_3/m$ using symmetry analysis of the parent $P6_3/mmc$ space group and taking into consideration the ED and NPD observations. The solution of the crystal structure was achieved by first analysing the isotopically exchanged H–D sample to located the positions of the O atoms of the water molecules, and then the deuterated sample to located the positions of the protons. The refinement of the intercalated D_2O molecules was carried out by the use of rigid bodies. In this approach we take advantage of the known shape of D_2O and we insert it into the lattice by defining a D–O–D torsion angle of 108° and a D–O bond length of 0.99 Å. In the Rietveld analysis only the centre of the molecule (in this case defined as the O atom) and the orientation of the protons with respect to the crystallographic axis are refined. During the course of the Rietveld analysis it was realized that there is a high degree of proton disorder, which we modelled as an additional D_2O molecule with the same centre as the first (placed at the O3 oxygen), but with different orientation angles. Anisotropic thermal parameters were also refined but constrained by the **TLS** matrices to take into account the librational and translational disorder (static or dynamic) of the D_2O. This approach produced a good agreement between
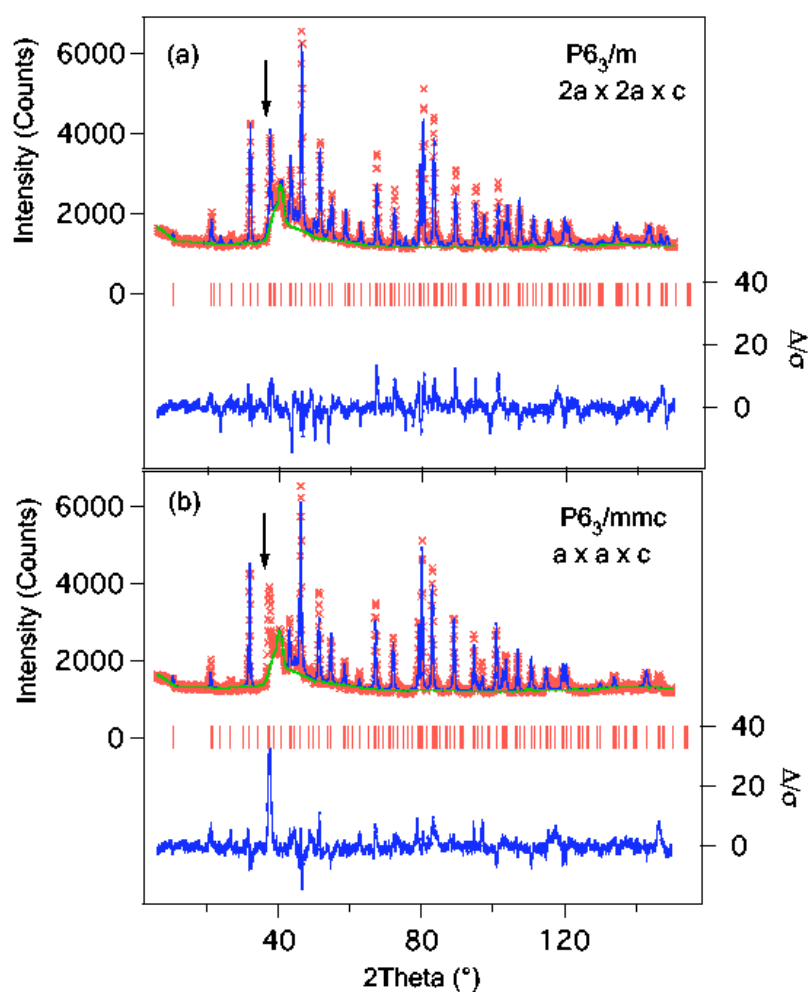
Figure 3. Rietveld refinement results from neutron powder diffraction data measured at 2 K from $Na_{0.35}CoO_2 \cdot yD_2O$. Here crosses represent the observations while a continuous line through the data is the calculated profile. Vertical lines represent the expected location of diffraction lines based on the unit cell and space group. The differences between the observation and the model (Δ), divided by the error (σ), are plotted at the bottom of the panel. The background was interpolated to include the broad feature at 40° for the analysis of all samples. In this figure it is shown as a solid line through the background of the data. (a) A Rietveld refinement using the $2a \times 2a \times c$ cell indicated by the ED measurements and space group $P6_3/m$. For this refinement the weighted profile agreement factor wR_p was 6.8%. (b) A Rietveld refinement using the model of Jorgensen *et al* [6]. The arrow indicates the location of the supercell reflections that is not accounted by the model of Jorgensen *et al*. For this model we obtained a wR_p of 8.5%.

our model and the NPD data, over the range of compositions, including the intensity of the reflections at 37° as shown in figure 3(a). Structural parameters and occupancies determined from all samples analysed using this model are given in table 2. In figure 3(b) we show the refinement of the same data using the Jorgensen model, which clearly does not account for the cell doubling reflection observed at 37°.

The main structural features of our model of superconducting $Na_xCoO_2 \cdot yD_2O$ are shown in figures 4 and 5. The structure of the CoO_2 sheets does not differ substantially from that

Table 2. Structural parameters determined from Rietveld analysis of our NPD data measured at 2 K. All Rietveld analyses were made using the double hexagonal cell, $2a \times 2a \times c$, in space group $P6_3/m$. In this setting of the structure there are two Co sites, Co1 $(0, 0, 0)$ and Co2 $(\frac{1}{2}, 0, 0)$. The O atoms that make up the CoO_2 sheets are O1 $(\frac{1}{3}, \frac{2}{3}, z)$ and O2 (x, y, z). The Na atom sites are Na1 $(0, 0, \frac{1}{4})$ and Na2 $(\frac{1}{3}, \frac{2}{3}, \frac{1}{4})$. The occupancies of the Na sites were constrained so that $f(Na1) + f(Na2)$ equals the Na content determined from NAA. In the Rietveld analysis D_2O was inserted as a rigid body, with a D–O bond length constrained to 0.99 Å and the D–O–D torsion angle set to 108°.

| $Co^{\alpha+}$	3.38	3.45	3.24	3.27
x	0.41	0.37	0.35	0.32
T_C (K)	2.8	2.5	4.7	4.5
a (Å)	5.6379(4)	5.6360(2)	5.6338(2)	5.6307(2)
c (Å)	19.4379(21)	19.5083(13)	19.5403(16)	19.7204(19)
O1 z	−0.0466(2)	−0.0472(2)	−0.0465(2)	−0.0480(2)
O2 x	0.1700(28)	0.1662(20)	0.1604(20)	0.1728(21)
O2 y	0.3367(24)	0.3330(19)	0.3327(19)	0.3333(19)
O2 z	0.0466(2)	0.0472(2)	0.0465(2)	0.0480(2)
Na1 f	0.29(1)	0.19(1)	0.21(1)	0.24(1)
Na2 f	0.12(1)	0.16(1)	0.14(1)	0.08(1)
O3 x	0.3420(31)	0.3715(23)	0.3482(23)	0.3243(25)
y	0.0181(26)	0.0099(22)	0.0371(22)	−0.0073(20)
z	0.1749(4)	0.1733(4)	0.1726(4)	0.1774(4)
f	1.28(3)	0.60(3)	1.22(3)	1.31(2)
D1 x	0.2765(63)		0.2762(51)	0.2662(49)
y	−0.1038(58)		−0.0811(56)	−0.1342(45)
z	0.1336(10)		0.1310(9)	0.1377(9)
f	0.58(2)		0.61(1)	0.62(1)
D2 x	0.2294(40)		0.2126(34)	0.2058(33)
y	0.1093(36)		0.0937(34)	0.0783(31)
z	0.1791(13)		0.1862(10)	0.1789(10)
f	0.58(2)		0.61(1)	0.62(1)
D3 x	0.2723(50)		0.2806(40)	0.2989(42)
y	−0.0417(67)		−0.0786(57)	−0.0735(59)
z	0.1271(7)		0.1304(10)	0.1295(6)
f	0.71(2)		0.60(1)	0.69(1)
D4 x	0.5456(31)		0.5502(24)	0.5233(27)
y	0.1013(37)		0.1104(31)	0.0774(33)
z	0.1741(11)		0.1761(9)	0.1889(9)
f	0.71(2)		0.60(1)	0.69(1)
y	1.28(3)		1.22(3)	1.31(3)
R_{wp} (%)	8.8	2.8	6.8	6.6
Co1–O2 (Å)	1.877(10)	1.868(8)	1.861(8)	1.881(8)
Co2–O1 (Å)	1.8628(22)	1.869(16)	1.8633(16)	1.8813(17)
Co2–O2 (Å)	1.849(12)	1.872(9)	1.89(9)	1.8559(9)
Co2–O2 (Å)	1.863(12)	1.869(9)	1.84(9)	1.908(11)
⟨Co–O⟩ (Å)	1.873(15)	1.860(11)	1.871(64)	1.889(12)
Na1–O3 (Å)	2.379(15)	2.552(11)	2.402(11)	2.336(13)
Na2–O3 (Å)	2.442(14)	2.37(11)	2.545(11)	2.348(11)

proposed by Takada [4]. To simplify the discussion of the Na and D_2O environment, we first consider an ideal structure of composition $x = \frac{1}{4}$ and $y = 1.5$ consisting of a fully occupied Na1 site surrounded by $6D_2O$ molecules in a triangular prism geometry (see figure 5(a)). Each
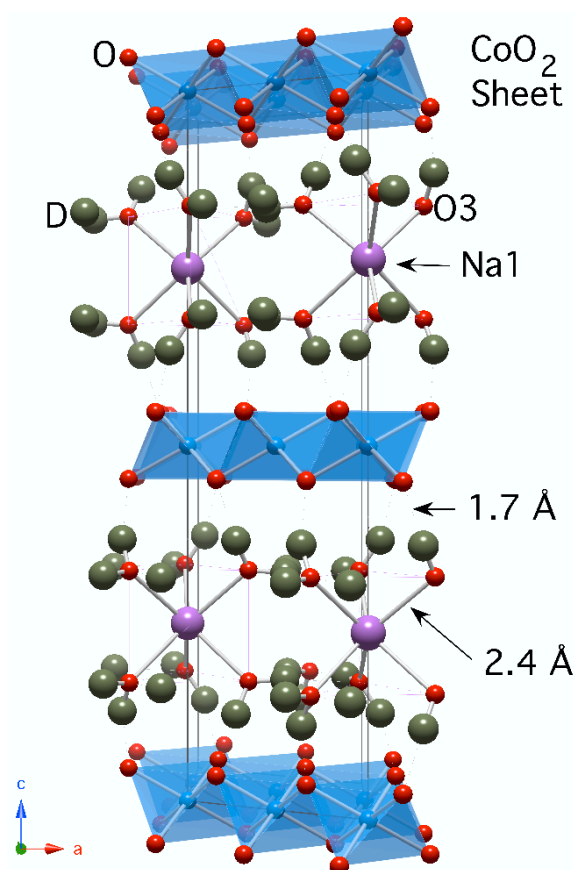
Figure 4. A three-dimensional representation of the structure of $Na_xCoO_2 \cdot yD_2O$ obtained from our Rietveld analysis. For simplicity we show only the Na1 site with the D_2O molecule centred at O3. The Na–O3 and D–O(–Co) bond lengths are shown.

NaO_6 prism consists of a Na atom in the centre of the prism and O atoms at each corner above and below the Na with Na–O bond lengths of 2.4 Å (figure 4). For this composition, NaO_6 prisms would be uncoupled from each other. This is a very typical coordination for Na in Na hydrate systems [11]. In such materials Na atoms are surrounded by H_2O forming *hydration shells*, with the O atom bonded to the alkali metal with a typical bond length of 2.4 Å, while the protons are pointing away from it [11]. The most common Na–H_2O coordination is 6, close to the value we find here. The doubling of a and b originates from this ordered arrangement of Na and its hydration shell (see figure 5). In fact, our NPD analysis has identified two Na sites centred at Na1 $(0, 0, \frac{1}{4})$ and Na2 $(\frac{1}{3}, \frac{2}{3}, \frac{1}{4})$. For Na rich compositions it is easy to see that additional Na (up to $x = \frac{1}{2}$) with the *same* coordination number can be accommodated into the ideal structure by the progressive filling of the Na2 sites, without a substantial rearrangement of the water molecules. For example the first sample we examined, $x = 0.35$, we find that the Na1 site is almost fully occupied with fractional occupancy $f = 0.21(1)$ (per formula unit), while the second Na2 site is significantly less populated with f 0.14(1) (Na1 + Na2 = 0.35). It is evident from inspection of table 2 that the Na1 site tends to be consistently more populated than the Na2 over the entire range of samples we have examined, while with decreasing x, the occupancies of the two Na sites decrease at similar rates. The coordination of O atoms around
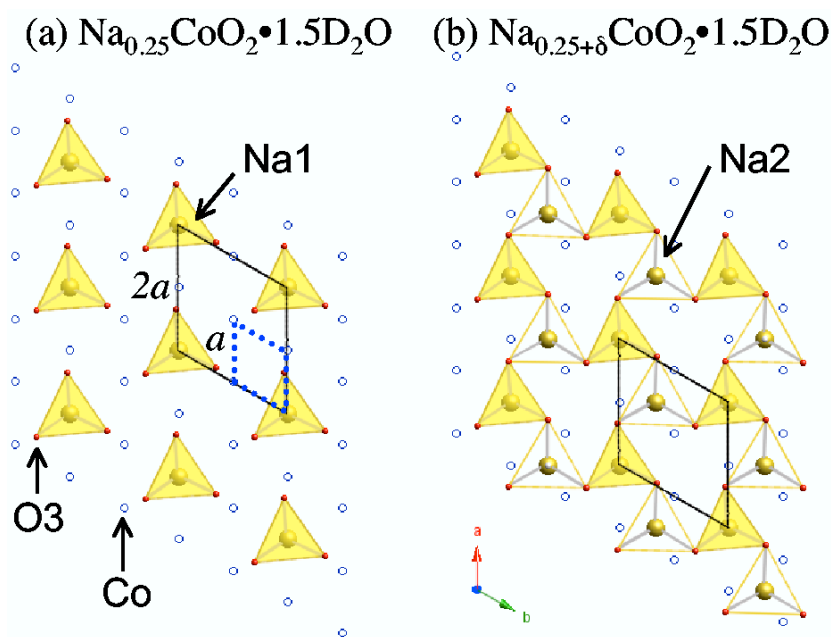
Figure 5. Projections of the Na-D_2O layer down the c-axis. The NaO_6 triangular prisms centred on Na are highlighted. The $2a \times 2a \times c$ unit cell is shown in solid lines and the $a \times a \times c$ cell as dashed lines. The doubling of the unit cell is evident from the position of the Na sites. D atoms are omitted for clarity. (a) The idealized $x = \frac{1}{4}$ structure. (b) A model for the $x = \frac{1}{2}$ structure with the Na2 site filled.

the Na2 site is naturally the same as in the Na1, such that NaO_6 prisms can be centred at either Na site. The samples used for neutron diffraction show that superconductivity is found over the range of $x = 0.41$–0.32, while the total amount of D_2O determined from our Rietveld refinements is $y \sim 1.3$, in good agreement with other reports [4, 12, 6, 5]. This suggests that Na content x can vary within a range ($\Delta x \sim 0.1$) while the amount of water y remains relatively unchanged. Finally our analysis shows that at least one of the protons of the D_2O molecule tends to point toward the CoO_2 sheets forming a hydrogen bond (D–O = 1.7 Å) with an O atom in that layer (figure 4). The structural model we employed in our best fits is slightly more complex than the one we just described, in that it includes two water molecules both centred at the O3 oxygen atom but with different orientations for the protons. This approach was employed to account for contributions of the possible coherent domains of the double hexagonal cell. More likely, however, this additional water molecule helps in modelling the large amount of disorder in the structure. See the appendix for a discussion of the orientation of the water molecules.

In our model the coordination of the O atoms of the D_2O molecules around Na atoms is triangular prismatic due to the mirror plane parallel to the ab-plane at $z = 1/4$. This coordination can be varied from prismatic to octahedral if the three oxygens on opposite sides of the Na atom along the c-axis are rotated with respect each other. This would indicate a loss of mirror symmetry that is not consistent with the ED measurements. To test the reliability of our model and the Na–O coordination that it imposes, we performed Rietveld refinements using space group $P6_3$, which would allow for octahedral coordinations of O atoms around Na as it removes the mirror plane parallel to the ab-plane. The results of this refinement showed

that the lowest *R*-factor was obtained for O positions that are mirrored about the Na layer confirming our original assignment of the space group of this phase. Indeed, refinements with starting points that give an octahedral coordination about the Na atom converged again on our original result.

The intercalation of H_3O^+ ions has been asserted to account for the difference between the expected Co valence if the system is doped by Na deficiency alone, and the one measured by redox titrations [7]. Recently we found that this difference between Co valence given by *x* and the measured Co valence follows a linear behaviour, with Na poor samples having the largest difference or the largest H_3O^+ content [9]. This trend is consistent with the notion that H_3O^+ resides on Na sites within the charge reservoir layer and acts as an additional doping defect [7]. However the model of the structure in which H_3O^+ ions reside on Na sites is not consistent with the NPD data. Indeed the placement of a H_3O^+ molecule on either of the Na sites leads to Rietveld refinements with a divergent χ^2. Simulations of NPD data based on the model of Takada *et al* [7] and accounting for different orientations of H_3O^+ bore little resemblance to our NPD measurements, and on this basis we can dismiss this model. The most likely location for H_3O^+ is residing within the hydrate layer between Na and CoO_2 sheets. Unfortunately the similarities between H_3O^+ and H_2O, as well as the static disorder in this system, make the unambiguous location of hydronium in this layer especially challenging using diffraction[5].

Finally we note that as the Co valence increases away from the optimal T_C region, the average Co–O bond length decreases, as seen from the tabulated Co–O in table 1. The decrease of the Co–O bond length is consistent with the removal of charge (addition of holes) from the CoO_2 sheets with respect to low spin Co^{3+}, t_{2g}^6. A similar behaviour has been noted for the anhydrous Na_xCoO_2 by Huang *et al* [13]. We further note that computation of the bond valence sums for the Co ions on the basis of these structural measurements also shows a positive slope with increasing Co valence, consistent with the removal of electrons from the CoO_2 sheets.

4. Discussion

The main conclusion that can be drawn from of our model, and the most relevant for the physics of this compound, is that $Na_xCoO_2 \cdot yH_2O$ is a homogeneous solid solution over a wide range of Na concentrations, rather than a point compound as suggested by Jorgensen *et al* [6]. This is indicated clearly by the fact that our series of superconducting samples crystallize in the same crystal structure while the Na content and Co valence state are varied. A second conclusion is that for the superconducting compositions, changes of Na content can be accommodated, within limits, by relatively small changes in the water content, as each O atom of the D_2O molecule will be coordinated locally to two Na atoms. In reality, a series of more or less stable ordered arrangements of Na2 occupied and vacant sites will occur for specific Na concentrations, although not all of them will be kinetically accessible. The complex synthesis route of this material (de-intercalation of Na and intercalation of water) helps to explain why more than one superstructure type is observed in the same sample. The inhomogeneous distribution of Na that is expected from de-intercalation produces a *disordered background* on which intercalated H_2O must arrange. The intercalation of water would yield some reorganization of the Na atoms at the local scale, but energetically a global rearrangement is too costly (unless an anneal is possible). As water is inserted into the lattice, local ordering of Na atoms occurs that resembles as much as possible the structure we describe. Fluctuations in the Na concentration are accommodated locally into the Na2 site, occasionally reaching an appropriate value for the formation of a long period superstructure. This model would

---

[5] In crystal systems H_3O^+ exhibits H–O bond lengths in the order of $\sim$0.87–0.97 Å, and three H–O–H torsion angles of approximately 102°, 105° and 118°; see [14–16].

account for the predominant doubling of the a-axis and the many other diverse superstructures observed by means of ED.

Our model of the structure of $Na_xCoO_2 \cdot yD_2O$ does fold onto the structural models proposed thus far [5, 6]. For example the Na1 site of the model given by Lynn *et al* maps onto the Na1 site of our model and similarly for the model of Jorgensen *et al* and the Na2 site. In fact our model and that of Jorgensen are similar in character in that they both describe a coordination of Na atoms with D_2O. The main difference is that we find a cell doubling arising from the ordering of Na atoms and the coordination of D_2O around the Na atoms is closer to 6, as opposed to 4 as suggested by Jorgensen [6]. We suggest that the models proposed by Jorgensen *et al* and Lynn *et al* to a large degree are ambiguous as their modelling of NPD data using a smaller $a \times a \times c$ cell results in a very high degree of atomic overlaps and degeneracies making it very difficult to draw a unique model. The significant degree of atomic overlap in these models describes the NPD data more in terms of a continuous scattering density in the hydration layers rather than consisting of discrete, non-overlapping atoms. In our work the cell doubling removes this ambiguity, at least partially, by unfolding the lattice and modelling the scattering density as discrete atoms with minimal atomic overlap arising from proton disorder.

Finally we comment on the proposal that the superconducting phase of $Na_xCoO_2 \cdot yH_2O$ is in fact a point compound that exhibits superconductivity at 5 K [6]. This suggestion appears to be strongly contradicted by our measurements. Our neutron diffraction measurements on these superconducting compounds clearly provide evidence of a solid solution, with the same phase appearing over a broad composition range, while the lattice constants vary accordingly. For a point compound we would expect a single phase to be present for the optimally doped composition, while, moving away from optimal doping, we would expect a mixed phase region with the superconducting phase always exhibiting lattice constants that are invariant with changing composition. Clearly this behaviour is not in agreement with our measurements, and further brings into question the predictions of the Jorgensen model. We note that the NPD data that have been measured over a large range of composition display the $(\frac{1}{2}, \frac{1}{2}, 0)$–$(\frac{1}{2}, \frac{1}{2}, 1)$ superlattice reflection pair attesting to the predominance and stability of this ordering.

5. Conclusion

In summary, our neutron and electron diffraction data have unravelled a new aspect of the structure of $Na_xCoO_2 \cdot yD_2O$, shedding light on its material and physical properties. We find that Na ions order leading to a doubling of the a-axis compared to the anhydrous compositions. The intercalation of water between Na and CoO_2 sheets leads to a structure where a NaO_6 triangular prism network networks forms, able to sustain a large range of x, allowing for the formation of a solid solution in which the electronic doping can be varied. A variety of sodium dopings, some of which lead to additional ordering, can be accommodated in the structure and should have little influence on the separation of CoO_2 sheets, as Na can be distributed over two sites that coordinate with one water molecule, while maintaining an average coordination close to the ideal Na–$6D_2O$. We further find that our neutron measurements are not consistent with a model in which H_3O^+ resides on Na sites, and we suggest that these ions form part of the hydrate layer between the Na and CoO_2 sheets.

Appendix

The structural model that we describe here accounts for the orientational disorder of the protons from the refinement of two sets of protons (D1, D2 and D3, D4) attached to the O3 oxygen. Although the constraints of D–O–D are rigid, the orientation and occupancy of these two sets

of protons were allowed to vary. These orientations share a common site as seen in the close proximity of the D1 and D3 protons, both pointing towards the CoO_2 layer. The D2 and D4 protons point in almost opposite directions to form a D2–O3–D4 torsion angle of 115°. The physical interpretation of this model would indicate that the orientation of the protons in the lattice, although disordered, on average assumes one of the two possible orientations that we present here. In both cases one of the protons (D1, D3) points towards an O atom in the CoO_2 layer forming a 1.7 Å H bond. In the first orientation the D2 proton points towards the O3 (2.3 Å) in the adjacent corner of the *same* triangular prism, while in the second orientation the D4 proton points towards an O3 oxygen in the *adjacent* prism, forming a D–O bond length of 2.1 Å. From the occupancies of the refinement the probabilities of the two orientations appear to be roughly equal, and an ordering of these two orientations forming a larger superlattice is possible.

References

[1] Wang Y, Rogado N S, Cava R and Ong N P 2003 *Nature* **65** 423
[2] Huang Q, Foo M L, Lynn J W, Zandbergen H W, Lawes G, Wang Y, Toby B H, Ramirez A P, Ong N P and Cava R J 2004 *Preprint* cond-mat/0402255
[3] Mukhamedchine I, Alloul H, Collin G and Blanchard N 2004 *Preprint* cond-mat/0402074
[4] Takada K, Sakurai H, Takayama-Muromachi E, Izumi F, Dilanian R A and Sasaki T 2003 *Nature* **421** 53
[5] Lynn J W, Huang Q, Brown C M, Miller V L, Foo M L, Schaak R E, Jones C Y, Mackey E A and Cava R J 2003 *Phys. Rev.* B **68** 214516
[6] Jorgensen J D, Avdeev M, Hinks D G, Burley J C and Short S 2003 *Phys. Rev.* B **68** 214517
[7] Takada K, Fukuda K, Osada I, Nakai M, Izumi F, Dilanian R A, Kato K, Takata H, Sakurai M, Takayama-Muromachi E and Sasaki T 2004 *J. Mater. Chem.* **14** 1448
[8] Schaak R, Klimczuk T, Foo M and Cava R 2003 *Nature* **424** 527
[9] Milne C J, Argyriou D N, Chemseddine A, Aliouane N, Veira J, Landsgesell S and Alber D 2004 *Phys. Rev. Lett.* **93** 247007
[10] Karppinen M, Asako I, Motohashi H and Yamauchi T 2004 *Chem. Mater.* **16** 1693
[11] Obst S and Bradaczek H 1996 *J. Phys. Chem.* **100** 15677
[12] Foo M *et al* 2003 *Solid State Commun.* **127** 33
[13] Huang Q, Foo M L, Lynn J W, Zandbergen H W, Lawes G, Wang Y, Toby B H, Ramirez A P, Ong N P and Cava R J 2004b *J. Phys.: Condens. Matter* **16** 5803
[14] Ng S W 1997 *Acta Crystallogr.* C **53** 633
[15] Mazumder G, De M, Mazumder S K and Mukhopadhyay A 2001 *Acta Crystallogr.* C **57** 562
[16] Van Brussel E M, Gossman W L, Wilson S R and Oldfield E 2003 *Acta Crystallogr.* C **59** o93